

Article

Absorption Coefficients of Phenolic Structures in Different Solvents Routinely Used for Experiments

Julia A. H. Kaeswurm ¹, Andreas Scharinger ², Jan Teipel ² and Maria Buchweitz ^{1,*} 

¹ Department of Food Chemistry, Institute of Biochemistry and Technical Biochemistry, University of Stuttgart, 70569 Stuttgart, Germany; julia.kaeswurm@lc.uni-stuttgart.de

² Chemisches und Veterinäruntersuchungsamt Karlsruhe, Weißenburger Str. 3, 76187 Karlsruhe, Germany; andreas.scharinger@cva.ka.de (A.S.); jan.teipel@cva.ka.de (J.T.)

* Correspondence: maria.buchweitz@lc.uni-stuttgart.de; Tel.: +49-71168569231

Abstract: Phenolic structures are of great interest due to their antioxidant properties and various postulated benefits on human health. However, the quantification of these structures in fruits and vegetables, as well as *in vivo* or *in vitro* experiments, is demanding, as relevant concentrations are often low, causing problems in exactly weighing the respective amounts. Nevertheless, the determination of used concentrations is often a prerequisite for accurate results. A possibility to quantify polyphenol is the use of UV/vis spectroscopy. Therefore, the absorption coefficients of selected phenolic structures were determined in three different solvents relevant for polyphenol research (water/methanol (50/50, v/v), water, and phosphate buffer at pH 7.5). To confirm the values based on weight and to avoid errors due to impurities, hygroscopic effects, and inadequate balance care, the mass concentrations were additionally determined by quantitative NMR (q-NMR). The coefficients presented in this article can help to quickly and easily determine accurate concentrations in a laboratory routine without wasting the often-precious standard compounds.

Keywords: polyphenols; anthocyanins; absorption coefficient; q-NMR



Citation: Kaeswurm, J.A.H.; Scharinger, A.; Teipel, J.; Buchweitz, M. Absorption Coefficients of Phenolic Structures in Different Solvents Routinely Used for Experiments. *Molecules* **2021**, *26*, 4656. <https://doi.org/10.3390/molecules26154656>

Academic Editor: Lucia Panzella

Received: 30 June 2021

Accepted: 27 July 2021

Published: 31 July 2021

Publisher's Note: MDPI stays neutral with regard to jurisdictional claims in published maps and institutional affiliations.



Copyright: © 2021 by the authors. Licensee MDPI, Basel, Switzerland. This article is an open access article distributed under the terms and conditions of the Creative Commons Attribution (CC BY) license (<https://creativecommons.org/licenses/by/4.0/>).

1. Introduction

For polyphenols and water-soluble secondary plant substances, many positive health effects have been proposed [1]. Besides identifying and quantifying phenolic structures in food [2–5], current research attempts to prove the postulated effects on human health have been performed by the use of *in vivo* and *in vitro* experiments [6–9]. Some previous investigations have focused on the holistic evaluation of the effects of polyphenolic extracts but not on the individual substances and their properties [10,11]. Our aim was to provide reliable data as a basis for further in-depth research into the quantification of individual phenolic structures and clarification of their interaction mechanisms. Quantification in biological samples and experiments into the effects and the biochemical mechanisms require stock solutions and dilutions with defined and precisely determined concentrations.

Particularly for physiologically relevant concentrations, the exact weighing is problematic. Isolated compounds might contain impurities of substances, which are not detectable by routinely applied methods such as HPLC-DAD-MS. In addition, commercially available phenolic standard compounds, with the exception of simple hydroxyl cinnamic acids, are cost-intensive and exhibit a limited shelf life in solution. Moreover, more hydrophobic phenolic structures can be dissolved in aqueous media (electrolyte solutions or buffers) only to a limited extent. Micro-balances fit to weigh sub-milligram amounts of substances are cost-intensive and require a strictly controlled environment. In addition, systematic errors can occur if they are not adequately maintained, serviced, and calibrated. Apart from general individual weighing errors, the lyophilized phenolic powders are often hygroscopic, which leads to corresponding weighing inaccuracies.

As polyphenols are aromatic substances, it is possible to determine their absorption at 280 nm by means of UV spectroscopy. According to the Bouguer–Lambert–Beer law, a substance's light absorption is proportional to its concentration in a given solvent; however, this is limited to a substance- and solvent-specific maximum concentration. Particularly, phenolic compounds tend to form supramolecular structures at higher concentrations in aqueous solutions [12], which limit the linear proportionality [13]. With the expansion of the conjugated π -electron system, the maximum absorption shifts from 280 nm to higher wavelengths (bathochromic effect). Furthermore, the wavelength might shift when different solvents are used, due to *pH*-dependent equilibria. Therefore, we determined absorption coefficients for some phenolic structures (Figure 1) in three different solvents: water, aqueous methanol (50/50 *v/v*), and aqueous phosphate buffer at *pH* 7.5 at λ_{\max} , the individual wavelength of maximum absorption, and at 280 nm for comparison.

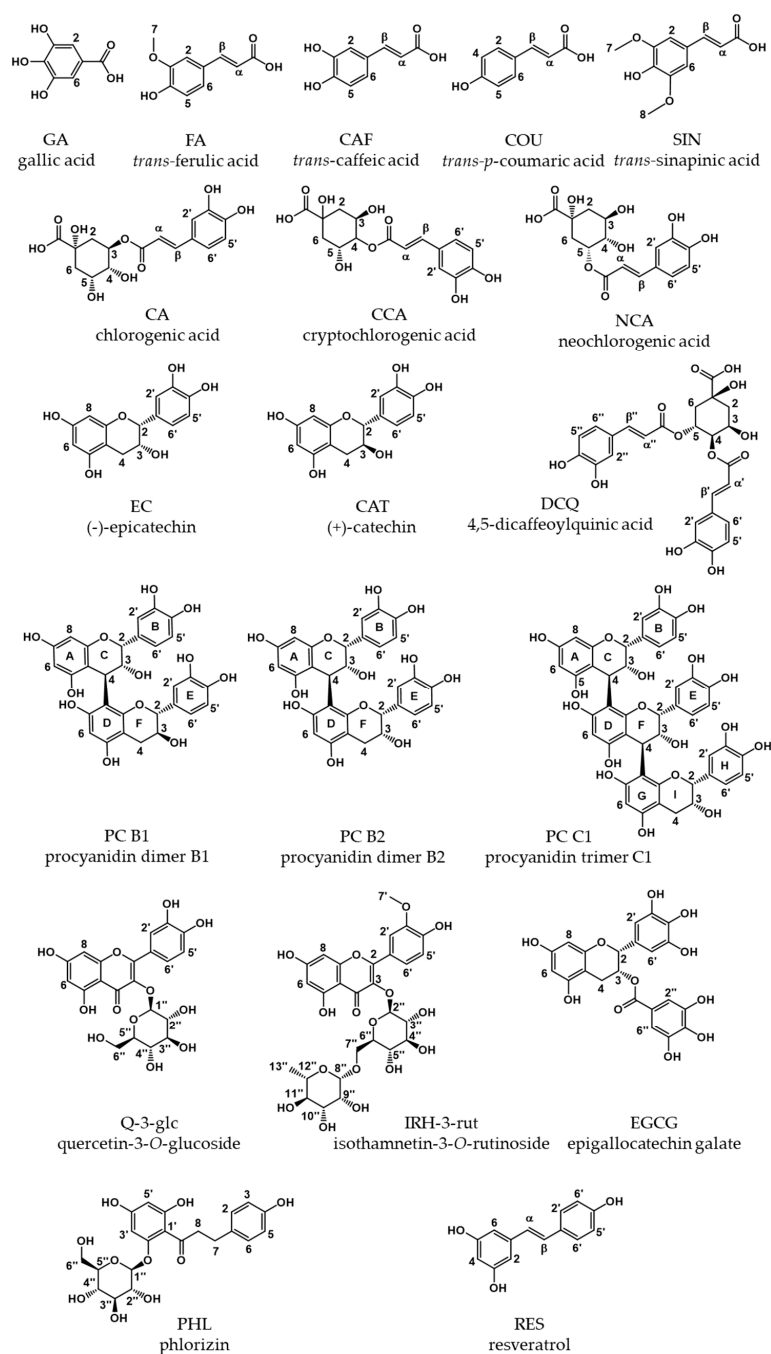


Figure 1. Overview of phenolic compounds investigated.

As the determination of absorption coefficients requires a reliable and confirmed concentration determination, we compared the data based on weight with concentrations determined by quantitative NMR (q-NMR). In recent years, q-NMR has been proven as a fast, reliable, sample saving and nondestructible absolute method to determine concentrations [14–17]. The quantifications performed by q-NMR are based on specific proton signals of the different substances.

2. Results

The following tables combine the results we found. Table 1 lists the extinction coefficients determined at the substances' individual wavelengths of maximum absorption (λ_{\max}). In Table 2 the extinction coefficients measured at the common wavelength $\lambda = 280$ nm are given. Table 3 shows the extinction coefficients determined in strongly acidic aqueous solution, both at λ_{\max} and at $\lambda = 280$ nm.

Table 1. Absorption coefficients at λ_{\max} (individual) for different phenolic compounds in methanol/water, water, and phosphate buffer pH 7.5 using concentrations determined by balance and q-NMR.

PP	Methanol/Water (50/50, v/v)						Water ^[a]						Phosphate Buffer pH 7.5						Difference of ϵ between Calculation Based on q-NMR and Balance ^[b] (%)			
	Balance			NMR			Balance			NMR			Balance			NMR						
	λ_{\max} /nm	ϵ /($L \cdot mol^{-1} \cdot cm^{-1}$)	ϵ /($L \cdot mol^{-1} \cdot cm^{-1}$)	λ_{\max} /nm	ϵ /($L \cdot mol^{-1} \cdot cm^{-1}$)	ϵ /($L \cdot mol^{-1} \cdot cm^{-1}$)	λ_{\max} /nm	ϵ /($L \cdot mol^{-1} \cdot cm^{-1}$)	ϵ /($L \cdot mol^{-1} \cdot cm^{-1}$)	λ_{\max} /nm	ϵ /($L \cdot mol^{-1} \cdot cm^{-1}$)	ϵ /($L \cdot mol^{-1} \cdot cm^{-1}$)	λ_{\max} /nm	ϵ /($L \cdot mol^{-1} \cdot cm^{-1}$)	ϵ /($L \cdot mol^{-1} \cdot cm^{-1}$)	λ_{\max} /nm	ϵ /($L \cdot mol^{-1} \cdot cm^{-1}$)	ϵ /($L \cdot mol^{-1} \cdot cm^{-1}$)				
GA	273	9507	±	436	9000	±	413	266	8021	±	166	7593	±	157	261	7406	±	288	7011	±	273	5.34
COU	309	18,279	±	1237	18,131	±	1227	290	17,867	±	301	17,722	±	298	287	16,216	±	187	16,084	±	186	0.81
CAF	322	15,458	±	590	14,792	±	565	315	14,606	±	601	13,976	±	575	312	12,073	±	266	11,553	±	255	4.31
FER	320	15,573	±	555	16,203	±	580	314	14,365	±	391	14,948	±	407	310	13,738	±	544	13,662	±	541	4.05
SIN	320	16,013	±	926	16,703	±	966	313	16,169	±	386	16,866	±	402	307	9743	±	510	10,163	±	532	4.31
CA	329	18,295	±	1435	18,091	±	1419	325	18,822	±	453	18,575	±	447	326	17,758	±	577	17,560	±	571	1.12
CCA	329	18,106	±	391	17,842	±	386	326	18,177	±	275	17,912	±	271	327	16,145	±	220	15,910	±	217	1.46
NCA	329	18,655	±	1084	18,323	±	1064	325	17,682	±	68	17,367	±	67	327	20,309	±	534	19,947	±	525	1.78
DCQ	330	34,027	±	1672	34,315	±	1686	325	30,331	±	612	30,587	±	617	328	29,988	±	1422	30,234	±	1431	0.85
CAT	280	4175	±	160	4047	±	155	280	3770	±	71	3655	±	69	280	3442	±	191	3337	±	185	3.06
EC	280	3981	±	73	3720	±	68	279	3771	±	83	3524	±	77	279	3714	±	157	3470	±	147	6.56
PC B1	281	7364	±	78	7534	±	80	280	7066	±	60	7229	±	62	280	6161	±	699 [c,e]	6302	±	715 [c,e]	2.30
PC B2	281	7496	±	223	7959	±	237	280	6810	±	83	7231	±	88	280	6698	±	189 [c]	7112	±	201 [c]	6.19
								280	7144	±	270 [d]			280	7026	±	198 [d]					
PC C1	281	11,542	±	802	15,397	±	1070	280	10,432	±	392	13,917	±	524	280	9783	±	533 [c]	13,051	±	711 [c]	33.40
EGCG	277	10,735	±	819	11,958	±	912	275	10,438	±	190	11,628	±	211	277	9525	±	255	10,610	±	284	11.39
IRH-	257	22,001	±	744	22,381	±	756	256	18,925	±	499	19,252	±	508	270	19,760	±	844	20,101	±	859	1.73
3-rut	357	19,075	±	646	19,404	±	657	353	15,850	±	415	16,123	±	422	362	14,216	±	618	14,461	±	629	1.73
Q-3-glc	258	19,568	±	938 ^[f]	25,053	±	1201	257	17,629	±	955 ^[f]	22,570	±	1223	269	17,545	±	368 ^[f]	22,464	±	471	28.03
RES	358	16,317	±	731 ^[f]	21,515	±	964	352	13,915	±	782 ^[f]	18,349	±	1031	365	12,009	±	215 ^[f]	15,836	±	283	31.86
	307	28,195	±	77	28,348	±	77	307	26,351	±	477	26,494	±	480	307	28,150	±	488 [c]	28,303	±	491 [c]	0.54
								307	25,455	±	874 [d]			307	28,340	±	492 [d]					
PHL	287	15,585	±	267	15,139	±	260	286	14,986	±	100	14,557	±	97	325	18,164	±	179	17,643	±	176	2.86

^[a] The respective pH values are provided in Table A1; ^[b] $(\epsilon_{q-NMR} - \epsilon_{balance}) / \epsilon_{balance} \times 100\%$; ^[c] the concentration of the solution was determined by UV spectroscopy with the absorption coefficient obtained in water; ^[d] the value is calculated with a second sample based on weight. ^[e] based on the values determined for PC B2, the values seem to be underestimated, ^[f] guaranteed purity is less than 90% (HPLC); therefore, the absorption coefficient might be underestimated. Due to unknown exact purity, the calculation is based on an estimated purity of 100%.

Table 2. Absorption coefficients at 280 nm for different phenolic compounds in methanol/water, water, and phosphate buffer *pH* 7.5 using concentrations determined by balance and q-NMR.

PP	Methanol/Water (50/50, <i>v/v</i>)				Water ^[a]				Phosphate Buffer <i>pH</i> 7.5				Difference of ϵ between Calculation Based on q-NMR and Balance ^[b] (%)												
	Balance		NMR		Balance		NMR		Balance		NMR														
	$\epsilon/(\text{L}\cdot\text{mol}^{-1}\cdot\text{cm}^{-1})$	\pm																							
GA	8635	\pm	521	\pm	8174	\pm	493	\pm	5901	\pm	595	\pm	5586	\pm	563	\pm	3703	\pm	98	\pm	3505	\pm	92	\pm	5.34
COU	14,035	\pm	471	\pm	13,921	\pm	467	\pm	15,982	\pm	548	\pm	15,852	\pm	544	\pm	15,470	\pm	162	\pm	15,344	\pm	160	\pm	0.81
CAF	10,491	\pm	564	\pm	10,039	\pm	540	\pm	12,376	\pm	550	\pm	11,843	\pm	526	\pm	11,722	\pm	247	\pm	11,217	\pm	237	\pm	4.31
FER	10,310	\pm	408	\pm	10,728	\pm	425	\pm	11,786	\pm	363	\pm	12,264	\pm	378	\pm	13,041	\pm	511	\pm	13,570	\pm	532	\pm	4.06
SIN	5894	\pm	365	\pm	6148	\pm	381	\pm	7985	\pm	718	\pm	8329	\pm	749	\pm	6042	\pm	310	\pm	6303	\pm	323	\pm	4.31
CA	8002	\pm	500	\pm	7913	\pm	494	\pm	10,119	\pm	264	\pm	9987	\pm	260	\pm	9231	\pm	262	\pm	9128	\pm	259	\pm	1.12
CCA	7893	\pm	189	\pm	7778	\pm	186	\pm	9176	\pm	138	\pm	9042	\pm	136	\pm	7942	\pm	127	\pm	7826	\pm	125	\pm	1.46
NCA	8544	\pm	477	\pm	8392	\pm	468	\pm	9189	\pm	69	\pm	9026	\pm	68	\pm	10,292	\pm	239	\pm	10,108	\pm	235	\pm	1.78
DCQ	14,961	\pm	669	\pm	15,087	\pm	675	\pm	15,644	\pm	341	\pm	15,776	\pm	343	\pm	15,188	\pm	562	\pm	15,317	\pm	567	\pm	0.85
CAT	4175	\pm	160	\pm	4047	\pm	155	\pm	3770	\pm	71	\pm	3655	\pm	69	\pm	3442	\pm	191	\pm	3337	\pm	185	\pm	3.06
EC	3981	\pm	73	\pm	3720	\pm	68	\pm	3754	\pm	83	\pm	3508	\pm	78	\pm	3702	\pm	159	\pm	3459	\pm	149	\pm	6.56
PC B1	7346	\pm	79	\pm	7515	\pm	81	\pm	7066	\pm	60	\pm	7229	\pm	62	\pm	6161	\pm	699 [c,e]	\pm	6302	\pm	715 [c,e]	\pm	2.30
PC B2	7482	\pm	227	\pm	7945	\pm	241	\pm	6810	\pm	83	\pm	7231	\pm	88	\pm	6698	\pm	189 ^[c]	\pm	7112	\pm	201 ^[c]	\pm	6.19
									7144	\pm	270 ^[d]						7026	\pm	198 ^[d]						
PC C1	11,518	\pm	802	\pm	15,366	\pm	1070	\pm	10,432	\pm	392	\pm	13,917	\pm	524	\pm	9783	\pm	533 ^[c]	\pm	13,051	\pm	711 ^[c]	\pm	33.40
EGCG	10,544	\pm	806	\pm	11,745	\pm	898	\pm	9970	\pm	197	\pm	11,106	\pm	219	\pm	9319	\pm	205	\pm	10,381	\pm	229	\pm	11.39
IRH-3- rut	8958	\pm	313	\pm	9112	\pm	319	\pm	8190	\pm	155	\pm	8331	\pm	158	\pm	13,588	\pm	587	\pm	13,823	\pm	597	\pm	1.73
Q-3- glc	7898	\pm	296 ^[f]	\pm	10,112	\pm	379	\pm	7474	\pm	452 ^[f]	\pm	9569	\pm	579	\pm	11,166	\pm	201 ^[f]	\pm	14,296	\pm	257	\pm	28.03
RES	13,731	\pm	150	\pm	13,805	\pm	151	\pm	13,483	\pm	217	\pm	13,556	\pm	218	\pm	13,889	\pm	184 ^[c]	\pm	13,964	\pm	185 ^[c]	\pm	0.54
									12,778	\pm	658 ^[d]						13,983	\pm	185 ^[d]						
PHL	14,187	\pm	229	\pm	13,781	\pm	223	\pm	13,940	\pm	83	\pm	13,541	\pm	81	\pm	8318	\pm	185	\pm	8080	\pm	180	\pm	2.86

^[a] The respective *pH* value is provided in Table A1; ^[b] $(\epsilon_{\text{q-NMR}} - \epsilon_{\text{balance}}) / \epsilon_{\text{balance}} \times 100\%$; ^[c] the concentration of the solution was determined by UV spectroscopy with the absorption coefficient obtained in water;

^[d] the value is calculated with a second sample based on weight. ^[e] based on the values determined for PC B2, the values seem to be underestimated. ^[f] guaranteed purity is less than 90% (HPLC); therefore, the absorption coefficient might be underestimated. Due to unknown exact purity, the calculation is based on an estimated purity of 100%.

Table 3. Absorption coefficients for different anthocyanins in potassium chloride buffer at *pH* 1 at 520 nm and λ_{\max} using concentrations determined by balance.

ACY	$\epsilon_{520\text{nm}}$ /(L·mol ⁻¹ ·cm ⁻¹)	λ_{\max} /nm	$\epsilon_{\lambda_{\max}}$ /(L·mol ⁻¹ ·cm ⁻¹)	ϵ According to [10]
PEL-3-glc	15,849 ± 2070	497	21,843 ± 2825	27,300
CYD-3-glc	25,526 ± 428	510	26,953 ± 464	26,900
DPD-3-glc	26,935 ± 680	516	27,087 ± 671	
PET-3-glc	26,821 ± 1386	516	26,892 ± 1353	
PEO-3-glc	23,926 ± 898	510	25,141 ± 931	
MLV-3-glc	27,911 ± 437	518	27,923 ± 443	28,000

3. Discussion

The absorption coefficients in methanol/water for COU, CAF, FER, and SIN are comparable with the values found by Rubach with 18,800, 15,800, 13,300, and 16,700 L·mol⁻¹·cm⁻¹, at λ_{\max} , respectively [18]. The structures of hydroxycinnamic acids are *pH*-dependent. In water, the *pH* values are concentration-dependent and range from 4.9 to 5.2 (Table A1). In buffer, the carboxylic group tends to dissociate, which explains the hypsochromic shifts in λ_{\max} and the decrease in absorption in phosphate buffer due to an increased formation of the negatively charged structures (Figure 2). The *pK_a* values, calculated by ChemAxon and listed in the HMDB data bank [19], are in a similar range with 4.00, 3.64, 3.77, and 3.61 for COU, CAF, FER, and SIN, respectively, and explain the increased bathochromic shifts. The values for the absorption coefficient calculated with a concentration based on balance or q-NMR are in a good agreement.

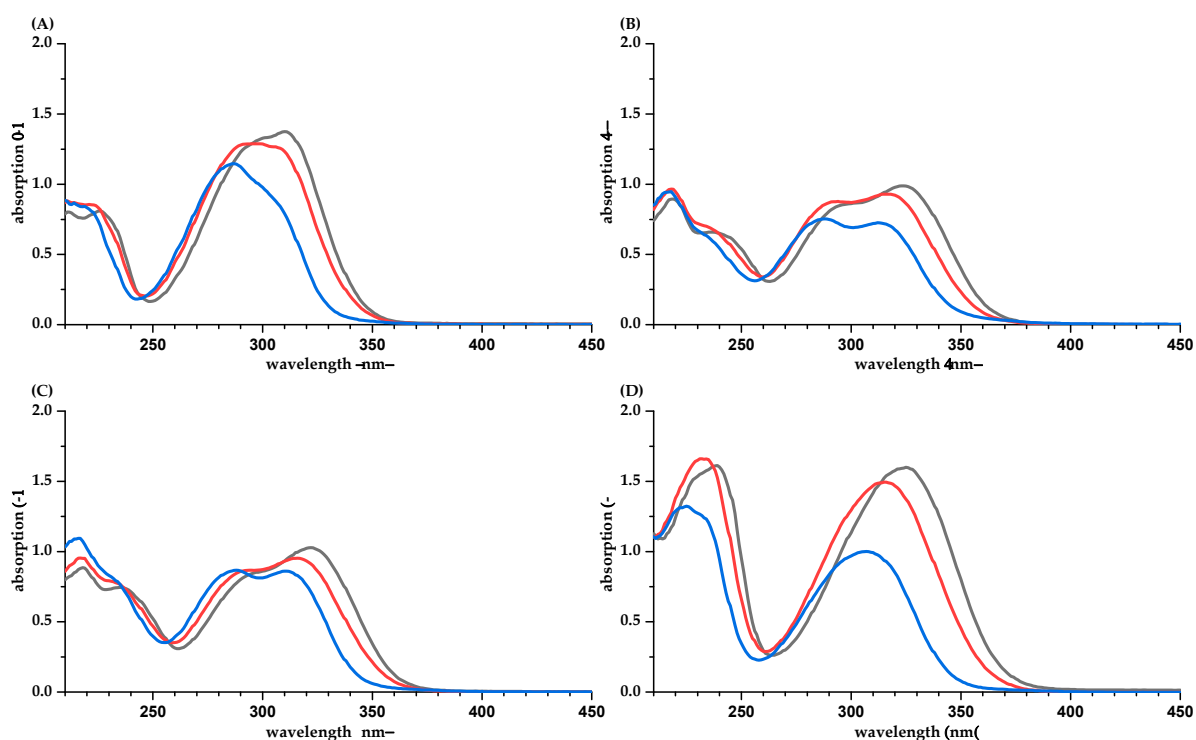


Figure 2. UV spectra of hydroxycinnamic acids in water/methanol (50/50, *v/v*, black), water (red), and phosphate buffer *pH* 7.5 (blue). (A), coumaric acid; (B), caffeic acid; (C), ferulic acid; (D), sinapinic acid. Concentrations are different for the four hydroxycinnamic acids but similar among the solvents.

The absorption coefficients for chlorogenic acid derivatives are independent of the ester position and the solvent (Tables 1 and 2, Figure 4A). Surprisingly, esterified with quinic acid, the absorption coefficient is roughly 25% higher compared to free CAF. The

significantly lower absorption at 280 nm underlines the importance to quantify these phenolic compounds separately at their individual absorption maxima or summarized at 320 nm. Our values determined in water and methanol/water are in good agreement with a former study by Rubach. Here, 19,500, 18,000, and 18,400 L·mol⁻¹·cm⁻¹ were found for chlorogenic (3'), neochlorogenic (4'), and cryptochlorogenic (5') acid [18]. The UV spectra of chlorogenic acids are not significantly influenced by the solution's *pH* values (Figure 4A). In water, the *pH* values of the isomers are significantly different, with 5.0 (CA), 4.6 (CCA), and 5.6 (NCA) (Table A1). However, the carboxylic group of the quinic acid with a *pK_a* of 3.3 [19] is widely distanced from the aromatic system, which is responsible for the absorption in the UV range. DCQ contains two independent CAF units and, therefore, the absorption should be doubled. However, the data are closer to the sum of the absorption of a chlorogenic acid and CAF.

Our values for CAT and EC are in agreement with the literature. A value of $\epsilon = 3988 \text{ L}\cdot\text{mol}^{-1}\cdot\text{cm}^{-1}$ has been reported for CAT and EC in methanol at 280 nm [20]. The absorption coefficients for the two dimers (PC B1 and B2) are in a similar range and are roughly doubled compared to the monomers. The trimer PC C1 follows the same trend comparing the data obtained by balance. In pure water and, in particular, in phosphate buffer, the absorption is reduced. In water, the *pH* value of all flavanols investigated is about *pH* 6 (Appendix A Table A1) and we interpret this more as an effect of the solvent's dielectric constant, than an effect of the *pK_a* (*pK_a* CAT/EC = 9) [19]. The q-NMR data of the procyanidins are suspicious. Due to the formation of rotamers, quantification of the procyanidins by NMR is hampered. Fortunately, in methanol/water, the sum of the signals for the six protons of the B- and E-ring and the two diastereomeric protons at position F 4 are suitable to quantify the dimers, ignoring the different ratios of the two rotamers [21,22] (Supplementary Material). For the trimer PC C1, the number of rotamers is even higher (up to 4) [22,23], significantly influencing signal intensity and, therefore, integration.

The UV spectra of the flavonoids IRH-3-rut and Q-3-glc show two maxima around 260 nm (B-ring) and around 360 nm (A and C-ring) (Figure 3). Gitelson et al. reported an absorption coefficient for quercetin-rutinoside of 25,400 L·mol⁻¹·cm⁻¹ at 358 nm in 80% aqueous methanol [24]. This is higher than the value of 21,515 ± 964 L·mol⁻¹·cm⁻¹ found in this study for Q-3-glc (based on q-NMR, Table 1). The absorption coefficient calculated with the mass concentration γ based on weight is markedly reduced. Due to the unknown purity of Q-3-glc and problems with precipitations, we rather trust the value based on NMR. The *pH* of the aqueous solution is 6.6 and 6.0 for IRH-3-rut and Q-3-glc, respectively. Both compounds have *pK_a* values of 6.4 [19], and an increased formation of the deprotonated structure is obvious, comparing the spectra in water and buffer at *pH* 7.5. The most acidic position is the hydroxyl group at position 7 (A-ring). However, due to mesomeric effects, the negative charge is transferred to position 4' in the B-ring and a bathochromic shift of λ_{max} is observed for both maxima.

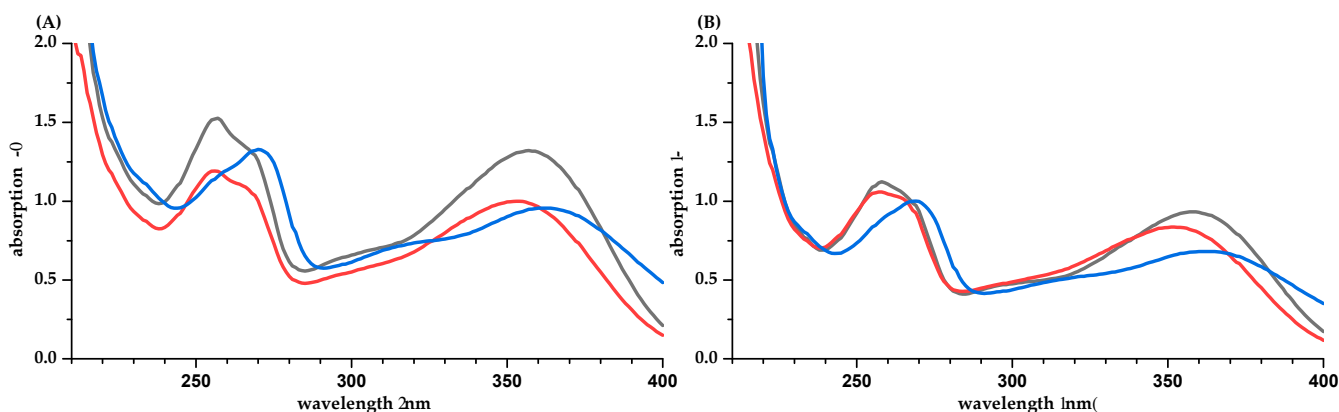


Figure 3. UV-spectra of IRH-3-rut (A) and Q-3-glc (B) in water/methanol (50/50, *v/v*, black), water (red), and phosphate buffer *pH* 7 (blue). Concentrations are different for the two flavonoids but similar between the solvents.

For EGCG (pK_a 7.99) [19], the UV absorption spectra in water (pH value is 6.0) and phosphate buffer are different (Figure 4B). However, the impact on the absorption coefficient is marginal. For PHL, a strong bathochromic shift and an increased absorption are observed in phosphate buffer (Figure 4C). This is due to the increased formation of the deprotonated, anionic PHL species (pK_a 7.87 [19], pH in water is 6.0).

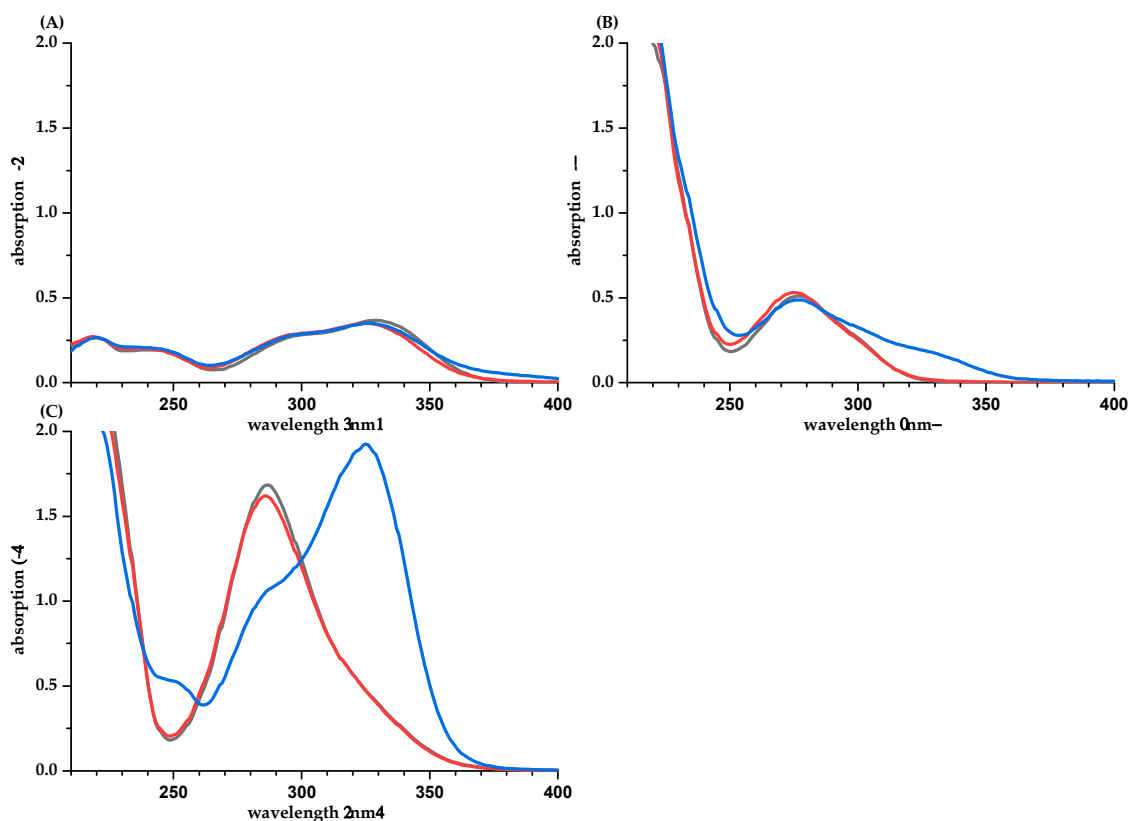


Figure 4. UV spectra of CA (A), EGCG (B), and PHL (C) in water/methanol (50/50, v/v , blue), water (orange), and phosphate buffer pH 7.5 (gray).

For anthocyanins, a wide variety of absorption coefficients are available in the literature, and some of them have been summarized by Giusti and Wrolstad [25]. However, the data vary in the wavelength of absorption and the solvent used. In particular, the pH value plays an important role for anthocyanins due to the pH -dependent equilibration between the red flavylium cation and the colorless hemiacetal. Therefore, pH values were checked for all anthocyanidin NMR dilutions to be $pH \leq 1.1$. Nevertheless, our values for the absorption coefficients differ significantly between the calculations based on the balance and q-NMR (16–40% higher in the calculation based on q-NMR, Table 3, Supplementary Material Table S1). Despite difficulties in weighing the hygroscopic anthocyanidins, we assumed a systematic underestimation by q-NMR. Data from the literature, in particular, the value of $26,900 \text{ L} \cdot \text{mol}^{-1} \cdot \text{cm}^{-1}$ for CYD-3-glc [25], support this. Therefore, we diluted two acidic (0.1% DCI) aqueous stock solutions of DPD-3-glc (1 g/mL, 1.6 g/mL) with potassium chloride buffer pH 1 and methanol- d_4 and determined the solutions' mass concentrations by q-NMR. A significant concentration difference (~20%) was observed between samples in buffer at pH 1 and acidic methanol- d_4 /D₂O (50/50, v/v) (Supplementary Material Table S2, Figure S1). Excluding the protons at position 6 and 8 (A-Ring), the mass concentration determined in methanol- d_4 /D₂O was similar to the mass concentration calculated by weight. Reduced integrals for protons at these positions have also been reported for other flavonoids [21].

The partial NMR excitation due to insufficient relaxation delay was checked by comparing spectra recorded with shorter vs. longer recycle delays and was found to be

irrelevant. Due to a sample *pH* below 1.1, the formation of significant amounts of hemiketals can also be excluded. It is conspicuous that the NMR resonances are broader in spectra obtained from buffered samples than in spectra from aqueous methanolic samples, this could be caused by self-association of the anthocyanidins in aqueous media. Such supramolecular aggregates are known to lead to reduced quantification due to the aggregates' slower tumbling rate (stochastic rotational and diffusion motion in the solution). The longer correlation times of such aggregates lead to faster T2 (spin-spin) relaxation and can induce signal broadening [26].

The focus of the investigation was aqueous solvents because *in vitro* experiments are usually performed in buffer. However, some polyphenols have limited solubility in water; therefore, HPLC-DAD standard stock solutions are often prepared in aqueous alcohol, and quantification with q-NMR also requires relatively high concentrations. Therefore, aqueous methanol was also included in the study. Despite limited solubility, stacking and hydration in aqueous solvents might be problematic for quantification. If the molecules form more than simple van der Waals interactions with the solvent, as with hydrogen bonds or (de-)protonation equilibria, NMR signal intensities may be influenced due to the carry-over of water presaturation into the molecule (NOE).

Supramolecular stacking has an impact on the absorption spectra and the absorption coefficient and on the NMR resonances, too. However, for the UV/vis spectra, this effect is negligible due to high dilutions (1:50–1:400, 1:10,000 for CA to measure absorptions in the range of 0.1–1.4); for NMR, we observed (as expected) signal broadening and lowered intensities, and these effects were inversely proportional to the sample temperature during measurement. However, due to the limited amounts of substances and due to their tendency to degrade, we did not systematically acquire spectra at $T(\text{sample}) > RT$.

4. Materials and Methods

4.1. Materials, Solvents, and Reagents

(-)-Epicatechin (EC) (95.1% purity HPLC), 3-*O*-caffeoylquinic acid (chlorogenic acid, CA) (99% titration with NaOH), 5-*O*-caffeoylquinic acid (neochlorogenic acid, NCA) (99.5% HPLC), phlorizin dihydrate (PHL) (99% purity), *trans*-sinapinic acid (SIN) (99.1% HPLC, 100.1% titration), and *trans*-ferulic acid (FER) (99.8% purity HPLC; 99.8% titration) were stored at room temperature. 4-*O*-caffeoylquinic acid (cryptochlorogenic acid, CCA) (99.6% HPLC) and epigallocatechin gallate (EGCG) (99% HPLC) were stored at 4 °C and quercetin-3-*O*-glucoside (Q-3-glc) (91.4% HPLC), as well as resveratrol (RES) (100% HPLC) at -20 °C. These phenolic structures were obtained from Sigma Aldrich (Darmstadt, Germany).

(+)-Catechin (CAT) (99.5% HPLC-PDA) and 4,5-*O*-dicafeoylquinic acid (DQA) (99.2% HPLC-PDA) were purchased from Phytolab GmbH & Co. KG (Germany) and stored at 4 °C. The procyanidins (PC) B1 (97.39%), B2 (96.72%), and C1 (97.41%), as well as *trans*-caffeic acid (CAF) (99.90% HPLC UV), *trans*-*p*-cumarinic acid (COU) (99.76% HPLC-UV), and isorhamnetin-3-*O*-rutinoside (IRH-3-rut) (99.06% HPLC-UV), were also purchased from Phytolab and stored at -80 °C (PCs) and room temperature, respectively.

The anthocyanin-3-*O*-glucosides cyanidin-3-*O*-glucoside (CYD-3-glc) (99.66% HPLC), delphinidin-3-*O*-glucoside (DPD-3-glc) (98.11% HPLC), malvidin-3-*O*-glucoside (MLV-3-glc) (99.10% HPLC), pelargonidin-3-*O*-glucoside (PLG-3-glc) (98.95% HPLC), peonidin-3-*O*-glucoside (PEO-3-glc) (98.79% HPLC), and petunidin-3-*O*-glucoside (PET-3-glc) (98.27% HPLC) were obtained as chlorides from Phytolab GmbH & Co. KG (Germany) and stored at -80 °C.

Na₂HPO₄ and NaH₂PO₄·H₂O were obtained from Roth (Karlsruhe, Germany) to prepare 100 mM of phosphate buffer at *pH* 7.5. Sodium hydroxide and hydrochloric acid (Grüssing, Germany) were used to adjust the *pH* value. For NMR experiments, D₂O and methanol-d₄ were purchased from Eurisotop (Saarbrücken, Germany), and the methanol used to dilute the samples for UV spectroscopy was acquired from Fisher Scientific (Loughborough, UK). All reagents and solvents were of analytical grade and ultrapure water (ELGA PurLab flex, Veolia Waters, Celle, Germany) was used throughout.

4.2. Preparation of the Stock Solutions

Polyphenols were weighed using an AT 20 (Mettler Toledo; Gießen, Germany) balance. Anthocyanin stock solutions were prepared in ultrapure water containing 0.1% HCl, and all other phenolic structures were dissolved in 0.5 mL of methanol- d_4 and subsequently mixed with 0.5 mL of D_2O . All solvents were degassed and samples were stored at $-20\text{ }^\circ\text{C}$. The compounds and mass concentrations (γ) determined by the balance and NMR are listed in Table 4.

Table 4. Mass concentration γ of the phenolic solutions based on the weights and determined with q-NMR at two different solutions.

PP	Quantification		γ_c /(mg/L)	γ_D /(mg/L) [b]	Average /(mg/L)	Difference between Balance/NMR (in %)	Literature for Signal Assignment	
	by Balance	by q-NMR spectroscopy						
	γ /(mg/L)	Protons Used for Quantification [a]						
GA	2368	H 2,6	2573	405	2502	± 36	5.6	[27]
COU	1158	H _b ; H 2,6; H 3,5; H _a	1219	186	1168	± 26	0.8	[28]
CAF	1088	H _b ; H 2; H 6; H 5; H _a	1164	185	1137	± 14	4.5	[28]
FER	1244	H _b ; H 2; H 6; H 5; H _a ; H 7	1251	190	1196	± 28	3.9	[29]
SIN	2094	H _b ; H 2,6; H _a ; H 7,8	2041	329	2008	± 17	4.1	[30]
CA	26,990	H _b ; H 2'; H 6'; H 5'; H _a	27,451	4523	27,295	± 78	1.1	[31]
CCA	2976	H _b ; H 2'; H 6'; H 5'; H _a	3016	504	3020	± 2	1.5	[32]
NCA	6096	H _b ; H 2'; H 6'; H 5'; H _a	6197	1036	6207	± 5	1.8	[31]
DCQ	3100	H _{b'} ; H 2'2''; H 6'6''; H 5'5''; H _{a'a''}	3088	510	3074	± 7	0.8	[33]
CAT	1502	H 2',5'; H6'; H 4 _{eq/ax}	1550	258	1549	± 1	3.1	[34]
EC	9362 [a]	H 2'; H 5',6'; H 4 _{eq/ax}	10,025	1669	10,020	± 3	7.0	[34]
PC B1	3954	H B 2',5',6' + E 2',5',6'; H F4 _{eq/ax}	3865				2.3	[22]
PC B2	5114	H B 2',5',6' + E 2',5',6'; H F4 _{eq/ax}	4816				5.8	[22]
PC C1	2492	H B 2',5',6' + E 2',5',6' + H 2',5',6'; H I4 _{eq/ax}	1868				25.0	[23]
EGCG	1144	H 2''6''; H 2'6'; H 4 _{eq/ax}	1036	509 [c]	1027	± 5	10.2	[27]
IRH-3- rut	1002	H 2'; H 6'; H 5'; H 13''	998	324 [d]	985	± 7	1.7	[35]
Q-3-glc	2576 [d]	H 2'; H 6'; H 5'; H 8; H 6	1954	345	2012	± 29	21.9	[36]
RES	1112 [d,e]	H 2',6'; H _b ; H 2,6; H 4	1144	178	1106	± 19	0.5	[37]
PHL	4679	H 2,6; H 3,5; H 3'; H _b	4817	798	4803	± 7	2.6	[38]

[a] for further information, see spectra provided in the Supplementary Material Figure S2, [b] dilution factor 6, [c] dilution factor 2, [d] pre-dissolved in 0.5 μL of DMSO- d_6 , [e] purity declaration was >90% (HPLC). The difference between balance and qNMR is reduced to 15% assuming a purity of 90% for the Q-3-glc standard compound.

4.3. Quantification Based on $^1\text{H-NMR}$

Absolute quantification of the polyphenols was performed in solution by quantitative nuclear magnetic resonance spectroscopy (qNMR) at the Chemical and Veterinary Investigation Office Karlsruhe (Chemisches Veterinär- und Untersuchungsamt, Karlsruhe, Germany). The measurement was carried out in methanol- d_4 / D_2O (50/50, v/v) for the initial concentration and an appropriate dilution to check for concentration-dependent impacts. Initially, anthocyanins were quantified at two different concentrations (1.2–2.3 mM, diluted 1:4 and 1:6) in 0.2 M potassium chloride buffer adjusted to $pH = 1$ with 0.2 M of HCl and D_2O . The pH value of the samples ranged between 1.05 and 1.10 after 1 h of equilibration. To investigate the systematic difference between the balance and qNMR, stock solutions of delphinidin-3-glucoside (D_2O , 0.1% DCI) were diluted in potassium chloride buffer $pH 1$ and acidic methanol- d_4 / D_2O (50/50, v/v , $pH 1$).

In general, the volume of 600 μL of the stock solutions was transferred into a 5 mm NMR tube and NMR spectra were recorded on a 400 MHz Bruker Avance (Bruker Biospin, Germany) equipped with a BBI 400S1 H-BB-D-05 Z probe and an automatic sample changer (Sample Xpress). Proton spectra were acquired using the pulse program noesygppr1d_d7

(1D NMR spectra) with presaturation of the water signal and an additional (fully passive) d7 delay limiting the presaturation irradiation to the d1 delay immediately before the excitation pulse. See Figure 5 as an example, for more spectra, see the Supplemental Material, Figure S2. To obtain an optimal and comparable excitation for all samples, the 90° pulse was calibrated for each sample using Bruker's PULSECAL routine. With a time domain (TD) of 128 k, 128 scans with 4 dummy scans were acquired, using a spectral width (SW) of 20.56 ppm (8223 Hz), an acquisition time (AQ) of 7.97 s, and a receiver gain (RG) of 32. Delay 1 (D1) and delay 7 (D7) were set to 4.00 and 60.0 s, respectively. The sample temperature was set at 300 K (± 0.1 K). All spectra were automatically phased and baseline-corrected. NMR spectra were analyzed using TopSpin version 4.06 (Bruker Biospin, Germany) and compound concentrations were determined using the PULCON principle (pulse length-based concentration determination) according to [14,39,40]. ^1H -NMR spectra of Quantification Reference solutions (QuantRef, = external standards), containing known, purity-corrected concentrations of the certified reference substances lactic acid and citric acid (aqueous QR for anthocyanins) or diethyl phthalate and 1,2,4,5-tetrachloro-3-nitrobenzene (organic QR for nonanthocyanin phenolic structures) were used to calculate the ERETIC factor according to Equation (1).

$$f_{ERETIC} = \frac{I_{\text{Ref}} \times SW_{\text{Ref}} \times M_{\text{Ref}}}{SI_{\text{Ref}} \times \gamma_{\text{Ref,corr}} \times N_{\text{H,Ref}} \times 1000} \left(\text{in } \frac{\text{a.u.} \times \text{ppm} \times \text{L}}{\text{mmol}} \right) \quad (1)$$

where:

I_{Ref} = absolute integral of the reference signal;

SW_{Ref} = spectral width;

M_{Ref} = molar mass;

SI_{Ref} = number of data points of the processed reference spectrum;

$\gamma_{\text{Ref,corr}}$ = mass concentration of reference substance, adjusted for purity;

$N_{\text{H,Ref}}$ = number of protons per reference molecule giving this resonance.

The following factor was used to quantify the anthocyanins according to Equation (2).

$$\gamma_{\text{An}} = \frac{I_{\text{An}} \times SW_{\text{An}} \times M_{\text{An}}}{SI_{\text{An}} \times f_{ERETIC} \times N_{\text{H,An}} \times f_{\text{dil}}} \times \frac{P_{\text{An}}}{P_{\text{Ref}}} \times \frac{NS_{\text{Ref}}}{NS_{\text{An}}} \left(\text{in } \frac{\text{mg}}{\text{L}} \right) \quad (2)$$

where:

γ_{An} = analyte mass concentration;

I_{An} = absolute integral of analyte in sample;

SW_{An} = spectral width;

M_{An} = molar weight of analyte;

SI_{An} = no. of data points of the processed analyte spectrum;

f_{ERETIC} = mean value ERETIC factor from QuantRef;

$N_{\text{H,An}}$ = number of protons per analyte molecule giving this resonance;

f_{dil} = dilution factor from analyte stock solution to measurement sample;

P_{An} = excitation pulse length used for the analyte sample (in μs);

P_{Ref} = excitation pulse length used for the QuantRef solution (in μs);

NS_{Ref} = number of recorded scans for the reference spectrum;

NS_{An} = number of recorded scans for the analyte spectrum.

Determination of the mass concentration γ was performed in duplicate and calculated as an average for the protons specified in Table 4. Signals for integration were selected having a low multiplicity and showing complete relaxation during the delay between the scans. The proton spectra are provided in the Supplementary Material.

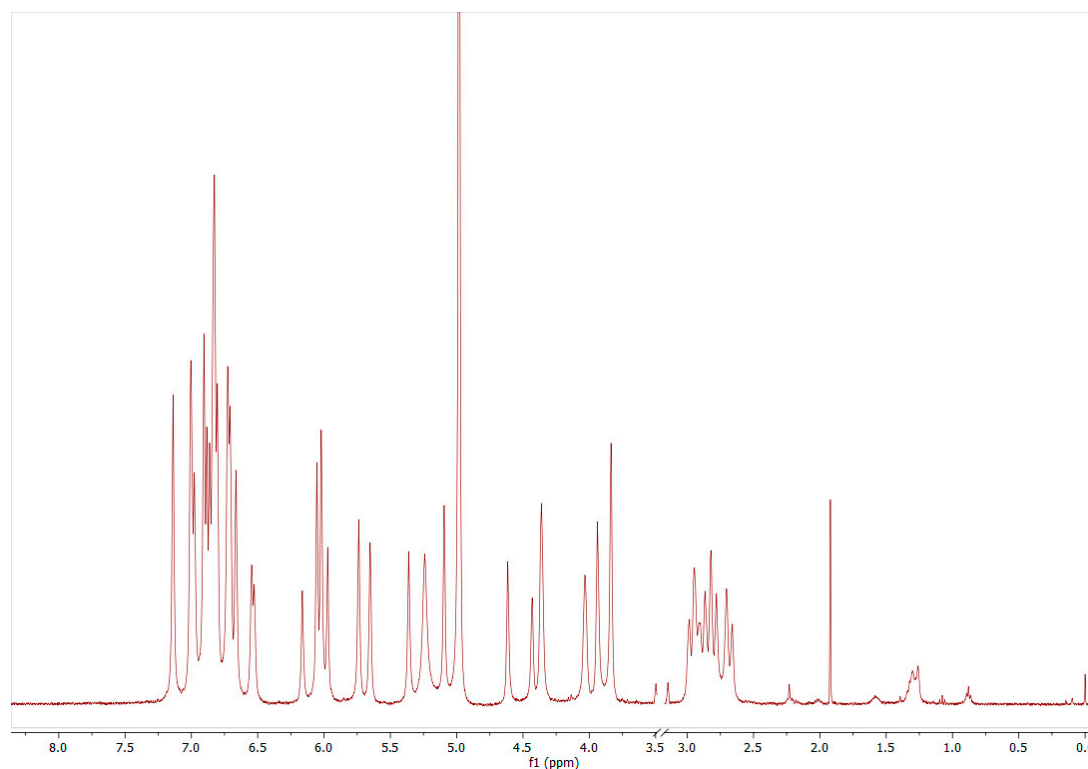


Figure 5. $^1\text{H-NMR}$ example spectrum of procyanidin-B2 (1868 mg/L) in methanol- $\text{d}_4/\text{D}_2\text{O}$ (50/50, v/v). The signals in the range of 6.5–7.15 ppm (the six protons of Ring B and E) and 2.6–3.0 ppm (the two diastereomeric protons F4) were used for summary quantification (Figure 1, $^1\text{H-NMR}$ spectra with signal assignments for all PP are provided in the Supplemental Material Figure S2, including references).

4.4. Determination of the Absorption Coefficient

The absorptions were determined in duplicate by UV/Vis spectroscopy (Spectrostar Nano, BMG, Labtech, Ortenberg, Germany, UV-Cuvette semi micro-cuvette $d = 1$ cm, Helma Analytics, Muehlheim, Germany) after equilibration for, at minimum, three different dilutions. The absorption coefficients ϵ (in $\text{L}\cdot\text{mol}^{-1}\cdot\text{cm}^{-1}$) were calculated according to Equation (3) for each concentration and then expressed as mean \pm standard deviation.

$$\epsilon = \frac{Abs \times f_{\text{dil}} \times M_{\text{an}}}{\gamma_{\text{an}} \times l \times 1000} \left(\text{in } \frac{\text{L}}{\text{cm} \times \text{mol}} \right) \quad (3)$$

Abs = absorption at λ_{max} or 280 nm;

M_{an} = molar weight of the anthocyanin;

γ_{an} = average mass concentration of the anthocyanin determined by q-NMR;

l = path length (1 cm);

f_{dil} = dilution factor;

1000 = conversion factor.

5. Conclusions

This article provides absorption coefficients for some phenolic structures in solvents generally used in experiments. The data also help to work with precise concentrations at low amounts during experiments and to save time and money. Commonly, it is recommended to use the absorption coefficients at λ_{max} ; however, due to equipment limitations, it might sometimes be required to use the coefficient obtained at 280 nm.

Supplementary Materials: Table S1: Absorption coefficients of anthocyanidin-3-glucosides calculated by mass concentration γ determined by balance and q-NMR in aqueous buffer at pH 1. Figure S1: Proton spectra recorded with a 400 MHz spectrometer and used for quantification, including signal assignment based on the literature of delphinidin-3-O-glucoside in buffer. Table S2: Mass concentration γ determined by q-NMR in acidic methanol/water (50/50, *v/v*) and potassium chloride buffer pH 1. Figure S2: Proton spectra recorded with a 400 MHz spectrometer and used for quantification, including signal assignment based on the literature and own 2D NMR spectra.

Author Contributions: Conceptualization, M.B.; methodology, M.B. and J.A.H.K.; investigation, J.A.H.K., A.S., J.T. and M.B.; resources, M.B.; data curation, J.A.H.K. and M.B.; writing—original draft preparation, J.A.H.K. and M.B.; writing—review and editing, A.S. and J.T.; visualization, J.A.H.K. and M.B.; supervision, M.B.; project administration, M.B.; funding acquisition, M.B. All authors have read and agreed to the published version of the manuscript.

Funding: This research was funded by the German Research Foundation (DFG), grant number 3811/1-1, by the Ministry of Science, Research and the Arts Baden-Württemberg (M.B., M. v. Wrangell program), the Dr. Leni Schöninger Foundation, and funds of the chemical industry, Germany (FCI).

Institutional Review Board Statement: Not applicable.

Informed Consent Statement: Not applicable.

Data Availability Statement: Not applicable.

Acknowledgments: Birgit Claasen is acknowledged for 2D-NMR spectra, particularly temperature-dependent spectra for PC 1, PC2, and C1, and valuable assistance in data interpretation and the analytical department of organic chemistry providing the micro-balance.

Conflicts of Interest: All authors declare that there is no conflict of interest.

Sample Availability: Not available.

Appendix A

Table A1. *pH* values for aqueous solution of the phenolic compounds in the specified concentration range.

PP	<i>c</i> /μM			<i>pH</i>		
GA	35	—	139	4.62	±	0.21
COU	18	—	71	4.92	±	0.24
CAF	15	—	60	4.96	±	0.18
FER	16	—	64	4.92	±	0.22
SIN	23	—	93	5.16	±	0.20
CA	8	—	38	5.00	±	0.36
CCA	21	—	84	4.62	±	0.30
NCA	17	—	86	5.64	±	0.08
DCQ	6	—	30	5.26	±	0.16
CAT	26	—	103	5.94	±	0.17
ECAT	81	—	323	6.10	±	0.11
PC B1	27	—	220	6.07	±	0.34
PC B2	25	—	197	6.13	±	0.08
PC C2	26	—	102	5.97	±	0.26
EGCG	6	—	50	6.02	±	0.01
IRH-3-rut	16	—	64	6.62	±	0.07
Q-3-glc	14	—	55	6.02	±	0.22
RES	9	—	37	6.33	±	0.44
PHL	27	—	107	6.01	±	0.03

References

1. Pandey, K.B.; Rizvi, S.I. Plant polyphenols as dietary antioxidants in human health and disease. *Oxid. Med. Cell. Longev.* **2009**, *2*, 270–278. [\[CrossRef\]](#)
2. Wojdyło, A.; Oszmiański, J.; Laskowski, P. Polyphenolic compounds and antioxidant activity of new and old apple varieties. *J. Agric. Food Chem.* **2008**, *56*, 6520–6530. [\[CrossRef\]](#)
3. Lin, L.-Z.; Harnly, J.; Zhang, R.-W.; Fan, X.-E.; Chen, H.-J. Quantitation of the hydroxycinnamic acid derivatives and the glycosides of flavonols and flavones by UV absorbance after identification by LC-MS. *J. Agric. Food Chem.* **2012**, *60*, 544–553. [\[CrossRef\]](#)
4. Scalbert, A.; Williamson, G. Dietary intake and bioavailability of polyphenols. *J. Nutr.* **2000**, *130*, 2073S–2085S. [\[CrossRef\]](#)
5. Jakobek, L.; García-Villalba, R.; Tomás-Barberán, F.A. Polyphenolic characterisation of old local apple varieties from Southeastern European region. *J. Food Compos. Anal.* **2013**, *31*, 199–211. [\[CrossRef\]](#)
6. Kaeswurm, J.A.H.; Claasen, B.; Fischer, M.-P.; Buchweitz, M. Interaction of Structurally Diverse Phenolic Compounds with Porcine Pancreatic α -Amylase. *J. Agric. Food Chem.* **2019**, *67*, 11108–11118. [\[CrossRef\]](#)
7. Buchweitz, M.; Kroon, P.A.; Rich, G.T.; Wilde, P.J. Quercetin solubilisation in bile salts: A comparison with sodium dodecyl sulphate. *Food Chem.* **2016**, *211*, 356–364. [\[CrossRef\]](#) [\[PubMed\]](#)
8. Williamson, G. The role of polyphenols in modern nutrition. *Nutr. Bull.* **2017**, *42*, 226–235. [\[CrossRef\]](#) [\[PubMed\]](#)
9. Chong, M.F.-F.; Macdonald, R.; Lovegrove, J.A. Fruit polyphenols and CVD risk: A review of human intervention studies. *Br. J. Nutr.* **2010**, *104*, S28–S39. [\[CrossRef\]](#)
10. Abate, G.; Zhang, L.; Pucci, M.; Morbini, G.; Mac Sweeney, E.; Maccarinelli, G.; Ribaud, G.; Gianoncelli, A.; Uberti, D.; Memo, M.; et al. Phytochemical Analysis and Anti-Inflammatory Activity of Different Ethanolic Phyto-Extracts of *Artemisia annua* L. *Biomolecules* **2021**, *11*, 975. [\[CrossRef\]](#)
11. Mastinu, A.; Bonini, S.A.; Premoli, M.; Maccarinelli, G.; Mac Sweeney, E.; Zhang, L.; Lucini, L.; Memo, M. Protective Effects of *Gynostemma pentaphyllum* (var. *Ginpent*) against Lipopolysaccharide-Induced Inflammation and Motor Alteration in Mice. *Molecules* **2021**, *26*, 570. [\[CrossRef\]](#)
12. Fernandes, A.; Brás, N.F.; Mateus, N.; de Freitas, V. A study of anthocyanin self-association by NMR spectroscopy. *New J. Chem.* **2015**, *39*, 2602–2611. [\[CrossRef\]](#)
13. Trouillas, P.; Sancho-García, J.C.; de Freitas, V.; Gierschner, J.; Otyepka, M.; Dangles, O. Stabilizing and Modulating Color by Copigmentation: Insights from Theory and Experiment. *Chem. Rev.* **2016**, *116*, 4937–4982. [\[CrossRef\]](#)
14. Teipel, J.C.; Hausler, T.; Sommerfeld, K.; Scharinger, A.; Walch, S.G.; Lachenmeier, D.W.; Kuballa, T. Application of ^1H Nuclear Magnetic Resonance Spectroscopy as Spirit Drinks Screener for Quality and Authenticity Control. *Foods* **2020**, *9*, 1355. [\[CrossRef\]](#) [\[PubMed\]](#)
15. Malz, F.; Jancke, H. Validation of quantitative NMR. *J. Pharm. Biomed. Anal.* **2005**, *38*, 813–823. [\[CrossRef\]](#)
16. Bharti, S.K.; Roy, R. Quantitative ^1H NMR spectroscopy. *Trends Anal. Chem.* **2012**, *35*, 5–26. [\[CrossRef\]](#)
17. Hatzakis, E. Nuclear Magnetic Resonance (NMR) Spectroscopy in Food Science: A Comprehensive Review. *Compr. Rev. Food Sci. Food Saf.* **2019**, *18*, 189–220. [\[CrossRef\]](#)
18. Rubach, K. Beitrag zur Analytik der Hydroxyczimtsäureester des Kaffees. Ph.D. Dissertation, Technische Universität Berlin, Berlin, Germany, 1969.
19. Wishart, D.S.; Tzur, D.; Knox, C.; Eisner, R.; Guo, A.C.; Young, N.; Cheng, D.; Jewell, K.; Arndt, D.; Sawhney, S.; et al. HMDB: The Human Metabolome Database. *Nucleic Acids Res.* **2007**, *35*, D521–D526. [\[CrossRef\]](#)
20. Kennedy, J.A.; Jones, G.P. Analysis of proanthocyanidin cleavage products following acid-catalysis in the presence of excess phloroglucinol. *J. Agric. Food Chem.* **2001**, *49*, 1740–1746. [\[CrossRef\]](#)
21. Tarascou, I.; Barathieu, K.; Simon, C.; Ducasse, M.-A.; André, Y.; Fouquet, E.; Dufourc, E.J.; de Freitas, V.; Laguerre, M.; Pianet, I. A 3D structural and conformational study of procyanidin dimers in water and hydro-alcoholic media as viewed by NMR and molecular modeling. *Magn. Reson. Chem.* **2006**, *44*, 868–880. [\[CrossRef\]](#) [\[PubMed\]](#)
22. Shoji, T.; Mutsuga, M.; Nakamura, T.; Kanda, T.; Akiyama, H.; Goda, Y. Isolation and structural elucidation of some procyanidins from apple by low-temperature nuclear magnetic resonance. *J. Agric. Food Chem.* **2003**, *51*, 3806–3813. [\[CrossRef\]](#)
23. Esatbeyoglu, T.; Jaschok-Kentner, B.; Wray, V.; Winterhalter, P. Structure elucidation of procyanidin oligomers by low-temperature ^1H NMR spectroscopy. *J. Agric. Food Chem.* **2011**, *59*, 62–69. [\[CrossRef\]](#) [\[PubMed\]](#)
24. Gitelson, A.; Chivkunova, O.; Zhigalova, T.; Solovchenko, A. In situ optical properties of foliar flavonoids: Implication for non-destructive estimation of flavonoid content. *J. Plant Physiol.* **2017**, *218*, 258–264. [\[CrossRef\]](#)
25. Giusti, M.; Wrolstad, R.E. Characterization and Measurement of Anthocyanins by UV-Visible Spectroscopy. *Curr. Protoc. Food Anal. Chem.* **2001**. [\[CrossRef\]](#)
26. Keeler, J. *Understanding NMR Spectroscopy*, 2nd ed.; Wiley: Chichester, UK, 2010; ISBN 978-0-470-74608-0.
27. Yuan, Y.; Song, Y.; Jing, W.; Wang, Y.; Yang, X.; Liu, D. Simultaneous determination of caffeine, gallic acid, theanine, (–)-epigallocatechin and (–)-epigallocatechin-3-gallate in green tea using quantitative ^1H -NMR spectroscopy. *Anal. Methods* **2014**, *6*, 907–914. [\[CrossRef\]](#)
28. Forino, M.; Tartaglione, L.; Dell’Aversano, C.; Ciminiello, P. NMR-based identification of the phenolic profile of fruits of *Lycium barbarum* (goji berries). Isolation and structural determination of a novel N-feruloyl tyramine dimer as the most abundant antioxidant polyphenol of goji berries. *Food Chem.* **2016**, *194*, 1254–1259. [\[CrossRef\]](#) [\[PubMed\]](#)

29. Anselmi, C.; Centini, M.; Maggiore, M.; Gaggelli, N.; Andreassi, M.; Buonocore, A.; Beretta, G.; Facino, R.M. Non-covalent inclusion of ferulic acid with alpha-cyclodextrin improves photo-stability and delivery: NMR and modeling studies. *J. Pharm. Biomed. Anal.* **2008**, *46*, 645–652. [[CrossRef](#)] [[PubMed](#)]
30. Cai, R.; Arntfield, S.D.; Charlton, J.L. Structural changes of sinapic acid and sinapine bisulfate during autoclaving with respect to the development of colored substances. *J. Am. Oil Chem. Soc.* **1999**, *76*, 433–441. [[CrossRef](#)]
31. Pauli, G.F.; Kuczkowiak, U.; Nahrstedt, A. Solvent effects in the structure dereplication of caffeoyl quinic acids. *Magn. Reson. Chem.* **1999**, *37*, 827–836. [[CrossRef](#)]
32. Nakatani, N.; Kayano, S.; Kikuzaki, H.; Sumino, K.; Katagiri, K.; Mitani, T. Identification, quantitative determination, and antioxidative activities of chlorogenic acid isomers in prune (*Prunus domestica* L.). *J. Agric. Food Chem.* **2000**, *48*, 5512–5516. [[CrossRef](#)]
33. Wu, C.; Chen, F.; Wang, X.; Wu, Y.; Dong, M.; He, G.; Galyean, R.D.; He, L.; Huang, G. Identification of antioxidant phenolic compounds in feverfew (*Tanacetum parthenium*) by HPLC-ESI-MS/MS and NMR. *Phytochem. Anal.* **2007**, *18*, 401–410. [[CrossRef](#)] [[PubMed](#)]
34. Da Silva, H.C.; Da Silva, A.N.R.; Da Rocha, T.L.S.; Hernandez, I.S.; Dos Santos, H.F.; de Almeida, W.B. Structure of the flavonoid catechin in solution: NMR and quantum chemical investigations. *New J. Chem.* **2020**, *44*, 17391–17404. [[CrossRef](#)]
35. Cao, X.; Wei, Y.; Ito, Y. Preparative Isolation of Isorhamnetin from *Stigma Maydis* using High Speed Countercurrent Chromatography. *J. Liq. Chromatogr. Relat. Technol.* **2009**, *32*, 273–280. [[CrossRef](#)] [[PubMed](#)]
36. Panda, S.; Kar, A. Antidiabetic and antioxidative effects of *Annona squamosa* leaves are possibly mediated through quercetin-3-O-glucoside. *Biofactors* **2007**, *31*, 201–210. [[CrossRef](#)]
37. Mattivi, F.; Reniero, F.; Korhammer, S. Isolation, Characterization, and Evolution in Red Wine Vinification of Resveratrol Monomers. *J. Agric. Food Chem.* **1995**, *43*, 1820–1823. [[CrossRef](#)]
38. Lommen, A.; Godejohann, M.; Venema, D.P.; Hollman, P.C.; Spraul, M. Application of directly coupled HPLC-NMR-MS to the identification and confirmation of quercetin glycosides and phloretin glycosides in apple peel. *Anal. Chem.* **2000**, *72*, 1793–1797. [[CrossRef](#)]
39. Wider, G.; Dreier, L. Measuring protein concentrations by NMR spectroscopy. *J. Am. Chem. Soc.* **2006**, *128*, 2571–2576. [[CrossRef](#)] [[PubMed](#)]
40. Monakhova, Y.B.; Kohl-Himmelseher, M.; Kuballa, T.; Lachenmeier, D.W. Determination of the purity of pharmaceutical reference materials by ¹H NMR using the standardless PULCON methodology. *J. Pharm. Biomed. Anal.* **2014**, *100*, 381–386. [[CrossRef](#)]